

LncRNA-OIS1 regulates DPP4 activation to modulate senescence induced by RAS

Li Li¹, Pieter C. van Breugel¹, Fabricio Loayza-Puch¹, Alejandro Pineiro Ugalde¹, Gozde Korkmaz¹, Naama Messika-Gold², Ruiqi Han¹, Rui Lopes¹, Eric P. Barbera³, Hans Teunissen⁴, Elzo de Wit⁴, Ricardo J. Soares⁵, Boye S. Nielsen⁵, Kim Holmstrøm⁵, Dannys J. Martínez-Herrera⁶, Maite Huarte⁶, Annita Louloui¹, Jarno Drost¹, Ran Elkon^{2,*} and Reuven Agami^{1,7,8,*}

¹Division of Oncogenomics, Netherlands Cancer Institute, Plesmanlaan 121, 1066CX Amsterdam, The Netherlands, ²Department of Human Molecular Genetics and Biochemistry, Sackler School of Medicine, 69978, Tel Aviv University, Tel Aviv, Israel, ³Division of Molecular Genetics, Netherlands Cancer Institute, Plesmanlaan 121, 1066CX Amsterdam, The Netherlands, ⁴Division of Gene Regulation, Netherlands Cancer Institute, Plesmanlaan 121, 1066CX Amsterdam, The Netherlands, ⁵Bioneer A/S, Kogle Allé 2, DK-2970 Hørsholm, Denmark, ⁶Institute of Health Research of Navarra (IdiSNA), 31008 Pamplona, Spain, ⁷Erasmus MC, Rotterdam University, 3000 CA Rotterdam, The Netherlands and ⁸Oncode institute, Netherlands Cancer Institute, Plesmanlaan 121, 1066CX Amsterdam, The Netherlands

Received November 01, 2017; Revised January 23, 2018; Editorial Decision January 27, 2018; Accepted January 29, 2018

ABSTRACT

Oncogene-induced senescence (OIS), provoked in response to oncogenic activation, is considered an important tumor suppressor mechanism. Long non-coding RNAs (lncRNAs) are transcripts longer than 200 nt without a protein-coding capacity. Functional studies showed that deregulated lncRNA expression promote tumorigenesis and metastasis and that lncRNAs may exhibit tumor-suppressive and oncogenic function. Here, we first identified lncRNAs that were differentially expressed between senescent and non-senescent human fibroblast cells. Using RNA interference, we performed a loss-function screen targeting the differentially expressed lncRNAs, and identified lncRNA-OIS1 (lncRNA#32, AC008063.3 or ENSG00000233397) as a lncRNA required for OIS. Knockdown of lncRNA-OIS1 triggered bypass of senescence, higher proliferation rate, lower abundance of the cell-cycle inhibitor CDKN1A and high expression of cell-cycle-associated genes. Subcellular inspection of lncRNA-OIS1 indicated nuclear and cytosolic localization in both normal culture conditions as well as following oncogene induction. Interestingly, silencing lncRNA-OIS1 diminished the senescent-associated induction of a nearby gene (Dipeptidyl Peptidase 4, DPP4) with established role

in tumor suppression. Intriguingly, similar to lncRNA-OIS1, silencing DPP4 caused senescence bypass, and ectopic expression of DPP4 in lncRNA-OIS1 knockdown cells restored the senescent phenotype. Thus, our data indicate that lncRNA-OIS1 links oncogenic induction and senescence with the activation of the tumor suppressor DPP4.

INTRODUCTION

Next-generation sequencing (NGS) and microarray technologies uncovered thousands of long non-coding RNAs (lncRNAs) encoded in the human genome (1,2). The majority of those lncRNAs are transcribed and processed in a similar manner to mRNAs, however, lack protein-coding potential (3,4). Although it is still unclear how many of those lncRNAs have a significant biological function, some of them have been found to be crucial players in the regulation of cellular processes such as proliferation, differentiation or development, as well as in a progression of a variety of human diseases including cancer (5–10). It has been shown that lncRNAs are key determinants of epigenetic regulation, modulation of chromatin structure, scaffolding or decoy function of mRNAs and post-transcriptional mRNA regulation (11–15). Gene regulation by lncRNAs can be a result of cis-action on nearby genes, or in trans by modulating mRNA stability, mRNA translation, or microRNA and RNA-binding-protein function (16–23).

*To whom correspondence should be addressed. Tel: +31 20 512 2079; Fax: +31 20 512 1999; Email: r.agami@nki.nl
Correspondence may also be addressed to Ran Elkon. Tel: +972 3 640 9038; Fax: +972 3 640 7471; Email: ranel@tauex.tau.ac.il

Cellular senescence was initially defined by Hayflick in 1965 as the limited lifespan of primary human fibroblasts in culture (24). It is a state of irreversible growth arrest which can be induced by different stimuli such as telomere shortening, DNA damage, oxidative stress or oncogene activation (25). Serrano *et al.*, were the first to observe that primary human and mouse fibroblasts enter senescence following the induction of oncogenic RAS, a process termed oncogene-induced senescence (OIS) (26). Cellular senescence has been studied most extensively as a strong tumor-suppressive mechanism against the emergence of oncogenes (27). Moreover, there is evidence indicating for a role of senescence in age-related conditions and diseases, including cancer, cardiovascular diseases, neurodegeneration, diabetes, sarcopenia and declining immune function in the elderly (28–32). In contrast, senescent cells can also contribute to tumorigenesis by secreting interleukins (e.g. IL-6, IL-8 and IL-1 α), metalloproteases (e.g. MMP-1 and MMP-3) and other cytokines (e.g. granulocyte-macrophage colony-stimulating factor (GM-CSF)), as part of the senescence-associated secretory phenotype (25,30,33–37). Therefore, senescence may either suppress or promote tumor progression depending on the context where it occurs (38,39). Given the impact of senescence on human physiology and pathology, it is of interest to understand the molecular mechanisms underlying senescence in order to utilize it for diagnosis and therapy.

A number of factors have been implicated in regulating senescence, including transcription factors, RNA binding proteins and microRNAs, such as p53, Ets (40), HuR (41), AUF1 (42) and TTP (43), and miR-377 (44), miR-22 (45). In contrast, despite increasing interest in the expression and function of lncRNAs, their possible implication in senescence remains largely unexplored. Recent works indicated a role of MIR31HG and SALNR in senescence (46,47), but a focused functional genetic screen was not described before. We therefore sought to identify senescence-associated lncRNAs using our established cellular system that induces senescence in primary human BJ fibroblasts (48). Using transcriptomic profiling we identified a number of differentially expressed lncRNAs following oncogene induction. Next, using functional screen, we discovered that one of the lncRNAs whose expression was induced upon oncogenic stress—lncRNA-OIS1—is required for OIS. We demonstrate that lncRNA-OIS1 is required for senescence by controlling a nearby DPP4 gene with a tumor suppressive activity. Collectively, our results provide a new lncRNA-mediated regulatory pathway for controlling DPP4 during OIS. Our findings support the role of lncRNAs as transcriptional regulators in critical processes such as cellular senescence and a potential role in cancer.

MATERIALS AND METHODS

Cell culture, transfection, retroviral and lentiviral transduction

BJ/ET/Ras^{V12}, TIG3/ET/RAS^{V12}, Ecopack 2 and HEK293-T cells were cultured in Dulbecco's modified Eagle's medium (Gibco), supplemented with 10% fetal calf serum (FCS) (Hyclone) and 1% penicillin/streptomycin (Gibco). Senescence was induced by treatment with 100

nM 4-OHT (Sigma) for 14 days. Retroviruses were made by calcium phosphate transfection of Ecopack 2 cells and harvest at 40 and 64 h later. Lentiviruses were made by polyethylenimine (PEI) transfection of HEK293T. Medium was refreshed after 16 h and collect the lentivirus by filtering through a 0.45 μ m membrane (Milipore Steriflip HV/PVDF) 40 h post-transfection and stored at -80°C . Cells were selected with the proper selection medium 48 h after transduction for at least 4 days until no surviving cells remained in the no-transduction control plate.

RNA-seq and analysis

RNA-seq samples were processed with TruSeq RNA library prep kit v2 (Illumina) and sequenced in a HiSeq 2500 (Illumina). Sequenced reads were aligned to the human genome (hg19) using TopHat2 (49) and gene expression levels were counted using HTseq (50) and normalized using quantile normalization. To avoid inflation of lowly expressed genes among the genes called as differentially expressed, we applied a dynamic cut-off which takes into account that technical variation varies with expression level. Specifically, in the comparison between two conditions, we divided the genes into 20 bins according to their average expression level, and calculated the standard deviation (SD) of fold-change within each bin. Genes whose expression was changed by at least 1.75-fold and this fold-change was above the bin's 1.75 SD (dashed curve in Figures 1B and 3B) were called as differentially expressed. To further avoid false positive calls among lowly expressed genes we set a floor level of five counts (i.e. any level below five was set to five). Functional enrichment analysis was done using DAVID (51). Global characterization of pathways that were deregulated upon knockdown of lncRNA-OIS1 was done using gene set enrichment analysis (GSEA) (52).

In situ hybridization

In situ hybridization (ISH) was performed using double-FAM labeled locked nucleic acid (LNA) probes (Exiqon) as described previously (53). Briefly, cells were fixed, permeabilized and pre-hybridized in hybridization buffer and then hybridized at 55°C for 1 h with LNA probes for lncRNA-OIS1: 5-TTGAAAACCCATCACTCCT-3, or with a scramble probe 5-TGTAACACGTCTATACGCCCA-3 as negative control, all at 25 nM. Cells were subsequently incubated with 3% hydrogen peroxide to block potential endogenous peroxidase, and then probes were detected with peroxidase-conjugated anti-fluorescein-Ab (Roche applied Sciences) diluted 1:400 followed by addition of Cy3-labeled TSA substrate for 10 min (Perkin Elmer). All cells were mounted with ProLong[®]GoldAntifade Mountant containing DAPI nuclear stain (ThermoFisher Scientific). Images were acquired using a Zeiss Axio Imager Z1 epi-fluorescence microscope equipped with an Axio-CamMRm CCD camera and a Plan-APOCHROMAT 63 \times /1.4 objective (Zeiss). Within the same experiment, images were acquired at the same exposure conditions.

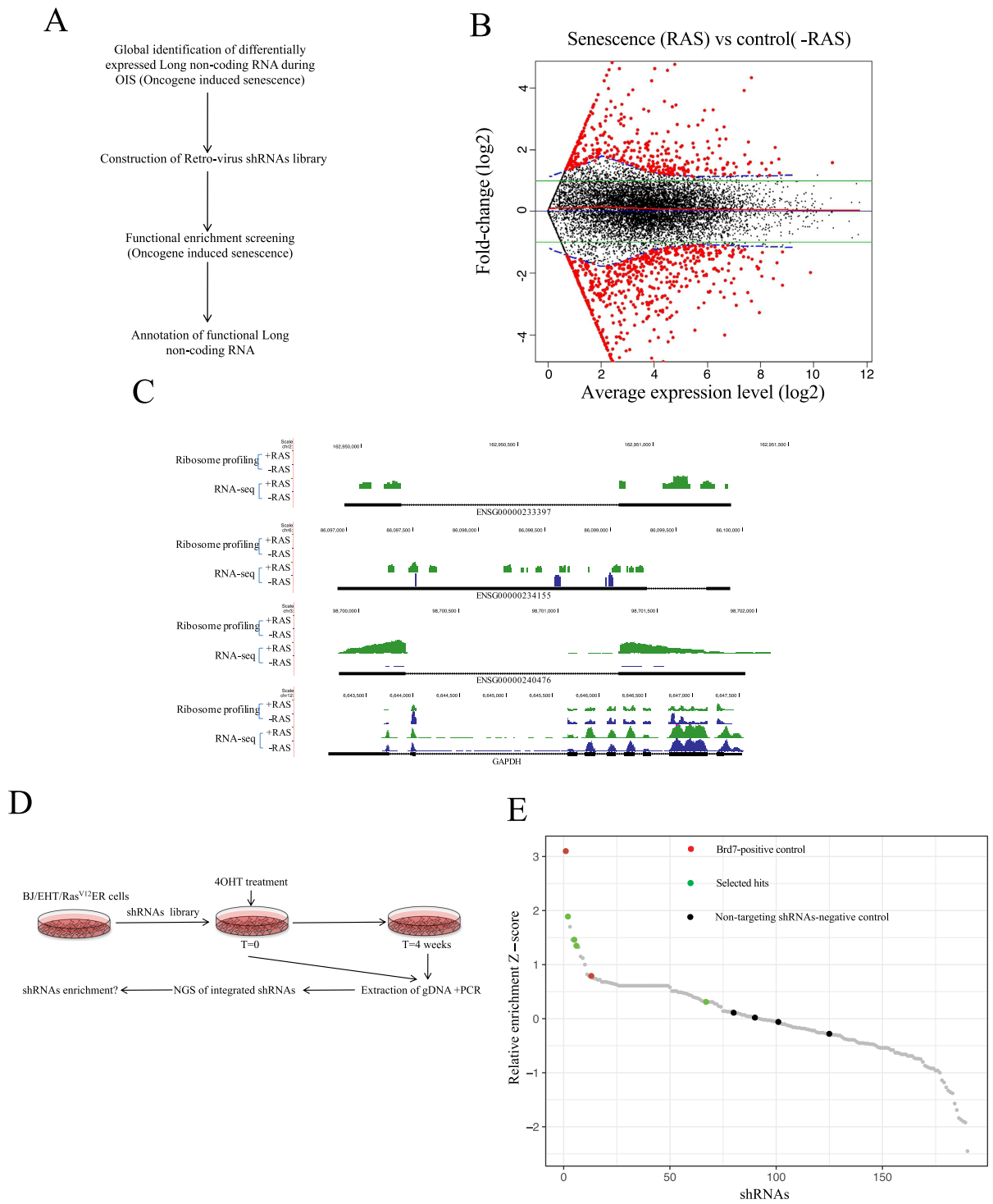


Figure 1. shRNAs screen identifies a lncRNA required for OIS. **(A)** A screening strategy of detecting functional lncRNAs. **(B)** RNA-seq comprehensively identified differentially expressed transcripts (mRNAs and lncRNAs) in senescent cells (treated with 4-OHT for 14 days) compared to untreated cells. **(C)** Ribosome profiling confirmed that the identified OIS lncRNAs have no protein coding capacity. Shown are selected examples and GAPDH as control. **(D)** The functional genetic screen procedure. NGS, next-generation sequencing. **(E)** Enrichment score calculated for each shRNA vector based on its prevalence in the pool, harvested after 4 weeks of tamoxifen (4-OHT) treatment (RAS^{V12} induction), relative to its prevalence in the T0 pool. The plot shows the distribution of standardized enrichment scores (Z-scores) for the entire shRNA library.

BrdU proliferation assay

BJ and TIG3 Cells were pulsed for 3 h with 30 μ M bromodeoxyuridine (BrdU, Sigma), washed two times with phosphate-buffered saline (PBS) and then fixed with 4% formaldehyde, wash two times with PBS and treated with 5M HCl/0.5% Triton to denature DNA and neutralized with 0.1M Na₂B₄O₇, incubated with anti-BrdU (Dako) for 2 h in RT after 30 min blocking with 3% bovine serum albumin (BSA) in 0.5% Tween PBS, washed in blocking buffer (PBS, Tween 0.5%, 3% BSA) three times, and finally incubated with FITC-conjugated anti-mouse Alexa FLOUR 488 secondary antibody (Dako) for 1 h, washed three times, stained with propidium iodide for 30 min. BrdU incorporation was measured by immunofluorescence (at least 300 cells were scored for each condition).

Senescence-associated β -galactosidase (SA- β -Gal) assay

BJ and TIG3 cells were transduced with different shRNAs constructs, plated in triplicate and treated with 100 nM 4-OHT for 14 days. β -galactosidase activity was determined by using the kit (Cell Signaling), and at least 300 cells were analyzed for each condition.

Ribosome profiling (Ribo-seq)

BJ Cells were treated with cycloheximide (100 μ g/ml) for 5 min, and lysed 20 mM Tris-HCl, pH 7.8, 100 mM KCl, 10 mM MgCl₂, 1% Triton X-100, 2 mM dithiothreitol (DTT), 100 μ g/ml cycloheximide, 1 \times complete protease inhibitor. Lysates were centrifuged at 1300 g and the supernatant was treated with 2 U/ μ l of RNase I (Invitrogen) for 45 min at room temperature. Lysates were fractionated on a linear sucrose gradient (7–47%) using the SW-41Ti rotor at 36 000 rpm for 2 h. Fractions enriched in monosomes were pooled and treated with proteinase K (Roche, Mannheim, Germany) in a 1% sodium dodecyl sulphate (SDS) solution. Released RNA fragments were purified using Trizol reagent and precipitated in the presence of glycogen. For libraries preparation, RNA was gel-purified on a denaturing 10% polyacrylamide urea (7 M) gel. A section corresponding to 30–33 nt, the region where most of the ribosome-protected fragments are comprised, was excised, eluted and ethanol precipitated. The resulting fragments were 3'-dephosphorylated using T4 polynucleotide kinase (New England Biolabs Inc. Beverly, MA, USA) for 6 h at 37°C in 2-(N-morpholino) ethanesulfonic acid (MES) buffer (100 mM MES-NaOH, pH 5.5, 10 mM MgCl₂, 10 mM β -mercaptoethanol, 300 mM NaCl). 3' adaptor was added with T4 RNA ligase 1 (New England Biolabs Inc. Beverly, MA, USA) for 2.5 h at 37°C. Ligation products were 5'-phosphorylated with T4 polynucleotide kinase for 30 min at 37°C. 5' adaptor was added with T4 RNA ligase 1 for 18 h at 22°C. The library was sequenced in illumina HiSeq2000 machine. The data were analyzed as described (54).

GRO-seq

Briefly, 5 \times 10⁶ nuclei were isolated and incubated 5 min at 30°C with equal volume of reaction buffer (10 mM Tris-Cl pH 8.0, 5 mM MgCl₂, 1 mM DTT, 300 mM KCl, 20

units of SUPERase In, 1% sarkosyl, 500 μ M adenosine triphosphate (ATP), Guanosine triphosphate (GTP) and Br-Uridine triphosphate (UTP), 0.2 μ M CTP+32P Cytidine triphosphate (CTP)) for the nuclear run-on. The reaction was stopped and total RNA was extracted with Trizol LS (Invitrogen) according to the manufacturer's instructions. RNA was fragmented using fragmentation reagents (Ambion) and the reaction was purified through p-30 RNase free spin column (BioRad). BrU-labeled RNA was immunoprecipitated with anti-BrdU agarose beads (Santa Cruz), washed one time in binding buffer, one time in low salt buffer (0.2 \times SSPE, 1 mM ethylenediaminetetraacetic acid (EDTA), 0.05% Tween-20), one time high-salt buffer (0.25 \times SSPE, 1 mM EDTA, 0.05% Tween-20, 137.5 mM NaCl) and two times in TET buffer (TE with 0.05% Tween-20). RNA was eluted with elution buffer (20 mM DTT, 300 mM NaCl, 5 mM Tris-Cl pH 7.5, 1 mM EDTA and 0.1% SDS) and isolated with Trizol LS. After the binding step, BrU-labeled RNA was treated with tobacco acid pyrophosphatase (Epicenter) to remove 5'-methyl guanosine cap, followed by T4 polynucleotide kinase (PNK; NEB) to remove 3'-phosphate group. BrU-containing RNA was treated with T4 PNK again at high pH in the presence of ATP to add 5'-phosphate group. The reaction was stopped and RNA was extracted with Trizol LS. Sequencing libraries were prepared using TruSeq Small RNA kit (Illumina) following manufacturer's instructions. Briefly, end-repaired RNA was ligated to RNA 3' and 5' adaptors, followed by RT-PCR amplification. cDNA was purified using Agencourt AMPure XP (Beckman Coulter) and amplified by polymerase chain reaction (PCR) for 12 cycles. Finally, amplicons were cleaned and size-selected using Agencourt AMPure XP (Beckman Coulter), quantified in a Bioanalyzer 2100 (Agilent), and sequenced in a HiSeq 2500 (Illumina). Sequenced reads were aligned to the human genome (hg19) using bowtie2 (55).

RNA isolation, reverse-transcription and quantitative real-time PCR (qPCR)

Total RNA was extracted by using TRIreagent (Bioline) reagent and following the manufacturer's protocol. cDNA was produced with SuperScript III (Invitrogen) using 4 μ g of total RNA per reaction. qPCR reaction was performed with SYBR green I Master mix in a LightCycler 480 (Roche). Primers used in qPCR are listed in Supplementary Table S5.

Western blot analysis

Whole-cell lysates were prepared as previously described (56). Membranes were immunoblotted with the following antibodies: CDKN1A (Sc-397, Santa Cruz; 1: 1000), HRAS (C-20, Santa Cruz; 1: 1000), DPP4 (ab28340, abcam; 1: 2000), GAPDH (Sc-47724, Santa Cruz; 1: 5000). Protein bands were visualized using corresponding secondary antibodies (Dako) and ECL reagent (GE Healthcare).

Chromosome conformation capture combined with sequencing (4C-seq)

Briefly, BJ cells were treated with or without 4-OHT for 14 days and 10^7 of cells for each condition were harvested and we performed 4C as previously described (57). An adapted two-step 4C-PCR was performed as previously described (58) to introduce template specific indexes. We had two viewpoints and used the following primers in the first PCR:

vp1_forward

AATGATACGGCGACCACCGAGATCTACACTCT
TTCCTACACGACGCTCTTCCGATCTCTTTGCTA
CTCTGTGAGATC

vp1_reverse

ACTGGAGTTCAGACGTGTGCTCTTCCGATCTA
TAGGGCTCTGGAGTCAG

vp2_forward

AATGATACGGCGACCACCGAGATCTACACTCT
TTCCTACACGACGCTCTTCCGATCTGTATTTCT
CTAGCTGGGATC

vp2_reverse

ACTGGAGTTCAGACGTGTGCTCTTCCGATCAA
CCGTAAAGTCTTCGCTC

We used the forward primers from the first PCR and combined the following reverse primers for the second PCR:

BJ – 4-OHT rep1

CAAGCAGAAGACGGCATAACGAGAT CGTGAT
GTGACTGGAGTTCAGACGTGTGCT

BJ – 4-OHT rep2

CAAGCAGAAGACGGCATAACGAGAT GCCTAA
GTGACTGGAGTTCAGACGTGTGCT

BJ + 4-OHT rep1

CAAGCAGAAGACGGCATAACGAGAT GGA
ACTGTGACTGGAGTTCAGACGTGTGCT

BJ + 4-OHT rep2

CAAGCAGAAGACGGCATAACGAGAT GCGGAC
GTGACTGGAGTTCAGACGTGTGCT

lncRNA-OIS1 expression analysis in tumors

Gene expression data was obtained from the TCGA Data Portal (<https://tcga-data.nci.nih.gov>). We selected those cancer types with transcriptome data available for at least five normal and five tumor samples, belonging to phenotypes ‘solid tissue normal’ and ‘primary solid tumor’, respectively. Lowly expressed genes (genes with raw read counts in less than half the normal samples and half the tumor samples) were removed within each cancer type data. Differential expression analysis was carried out with R/Bioconductor package limma (59) using voom normalization (60). Pearson correlation calculation was carried out using normalized gene expression values, also in R/Bioconductor.

RESULTS

Genome-wide identification of lncRNAs responsive to OIS

To identify lncRNAs with a role in OIS, we used the model of primary human BJ fibroblasts expressing hTERT and 4-OH-tamoxifen (4-OHT)-inducible oncogenic H-Ras^{V12} (BJ/ET/Ras^{V12}ER cells) (48). RNA sequencing (RNA-

seq) in senescent cells and non-senescent control cells revealed senescence-associated differentially expressed transcripts (Figure 1B). Of those transcripts, we found 34 and 6 lncRNAs upregulated and downregulated respectively during OIS (Supplementary Table S1). Ribosome profiling confirmed the non-coding nature of these RNAs (Figure 1C). We also confirmed by qRT-PCR the induction of some lncRNAs following H-Ras^{V12} induction (Supplementary Figure S1A).

A focused loss-of-function screen for lncRNAs required for OIS identifies lncRNA-OIS1.

To examine possible causal roles for lncRNAs in OIS, we developed RNAi tools to target the 40 lncRNAs that were differentially expressed in OIS. We generated a pooled library consisting of five different shRNAs against each lncRNA, and included four non-targeting shRNAs as negative controls, as well as two positive control shRNAs targeting BRD7—a gene identified as a tumor suppressor in OIS (48) (Supplementary Table S2). We transduced cells with three independent retroviral pools of the shRNAs library, and following puromycin selection harvested half of each cell population as control (T0, Time 0). We cultured the rest of the cells with 4-OHT treatment for 4 weeks, then harvested the cells (T4, Time 4 weeks) and performed NGS to identify shRNAs enriched in the final populations (T4) compared to the initial (T0) pool (Figure 1D).

Our screen detected the positive control shRNAs against BRD7, as well as few shRNAs targeting different lncRNAs enriched in the RAS-induced cell populations, suggesting that the knockdown of these lncRNAs conferred a growth advantage in BJ/ET cells expressing Ras^{V12} (Figure 1E). For further validation, we selected two hits: lncRNA#32, which has one shRNA (shRNA3) at the top of the enrichment list in all three replicates, and another shRNA (shRNA2) giving minor enrichment; and lncRNA#30 with two shRNAs (shRNA5 and shRNA3) showing consistent enrichment in all three replicates (Figure 1E and Supplementary Table S3). We validated the hits by repeating the OIS experiment using individual shRNAs. We used an shRNA targeting BRD7 (BRD7_shRNA4) as a positive control, and two non-targeting shRNA as negative controls. A proliferation assay (using BrdU labeling) indicated bypass of oncogene-induced cellular arrest by one shRNA (#30–5) targeting lncRNA#30 and two shRNAs (#32–2 and #32–3) targeting lncRNA#32 (Figure 2A and Supplementary Figure S2A). To further examine the effect of loss-of lncRNA#30 and #32 in OIS, we measured the induction of senescence-associated β -galactosidase (SA- β -Gal). In comparison with negative control cells, a marked decrease in SA- β -Gal was observed in Ras^{V12}-expressing BRD7-knockdown (BRD7 kd), lncRNA#30–5 and lncRNA#32–2 and #32–3 cells (Figure 2B and Supplementary Figure S2B). In contrast, shRNA (#30–3) was not validated as expected from the screen outcome. Interestingly, RNA expression analysis indicated that only shRNAs #30–5, #32–2 and #32–3 were effective toward their lncRNA targets, suggesting on-target activity (Figure 2C and D). To exclude off-target effects of the shRNAs, we designed additional vectors targeting lncRNA#30 and #32 (Supplementary Table

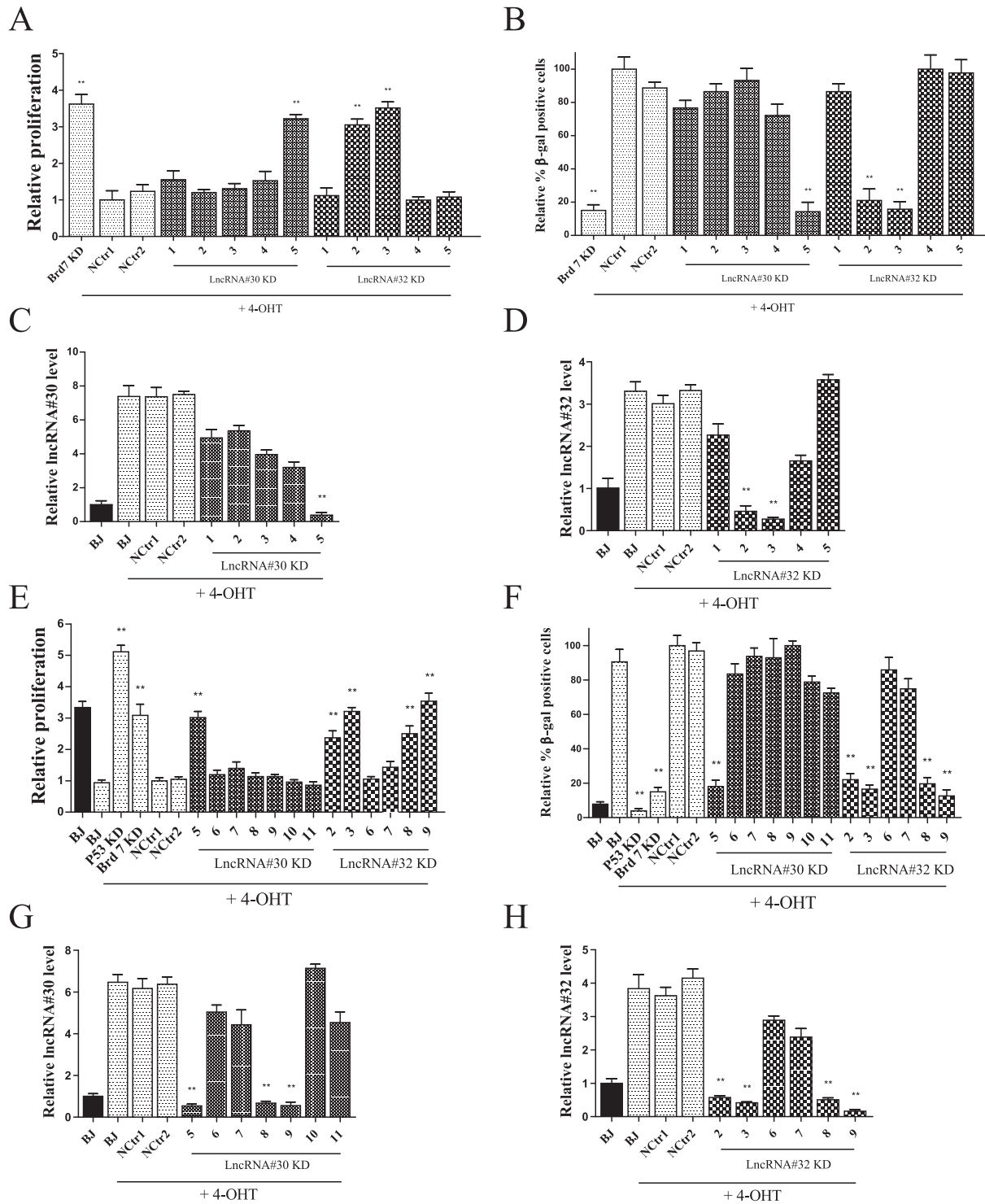


Figure 2. Functional validation of selected lncRNAs. (A) The proliferation of the various shRNA-transduced BJ-RAS^{V12} cells was quantified using BrdU assay, $**P < 0.0005$, two-tailed Student's *t*-test. For every condition, the percentage of BrdU-positive cells was normalized to negative control cells. (B) Senescent cells were quantified using SA-β-Gal assay, $**P < 0.0005$, two-tailed Student's *t*-test. For every condition, the percentage of β-gal-positive cells was normalized to negative control cells. (C and D) qRT-PCR analysis of lncRNA#30 and #32 in the various shRNA-transduced cells treated with 4-OHT relative to untreated cells. Data were normalized to a housekeeping gene and the levels in untreated cells was set to 1, $**P < 0.0005$, two-tailed Student's *t*-test. (E and F) Validation of additional shRNA-transduced BJ-RAS^{V12} cells was performed as in panel A and B. BrdU ($**P < 0.001$) and SA-β-Gal assays ($**P < 0.0005$) were quantified by two-tailed Student's *t*-test. (G and H) qRT-PCR analysis of lncRNA #30 and #32 in the shRNA-transduced cells presented in E and F. Data were normalized to a housekeeping gene and the levels in untreated cells was set to 1, $**P < 0.0005$, two-tailed Student's *t*-test.

S6), and repeated the proliferation and SA- β -Gal assays. This experiment identified more functional shRNAs (#32–8, #32–9) targeting lncRNA#32, but no additional shRNAs targeting lncRNA#30 (Figure 2E and F; Supplementary Figure S3A and B). qRT-PCR confirmed loss-of expression of lncRNA#32 by all four active shRNA vectors (#32–2, 3, 8 and 9) (Figure 2H). In contrast, two new shRNAs (#30–8, #30–9) showed efficient loss-of lncRNA#30 (Figure 2G) but did not induce bypass of OIS (Figure 2E and F; Supplementary Figure S3A and B), indicating that the bypass of OIS by shRNA#30–5 was not mediated by its targeted lncRNA. Altogether, these results demonstrate that lncRNA#32 is both induced by oncogenic RAS and is required for the establishment of the OIS phenotype.

To further solidify the role of lncRNA#32 in OIS we made use of a dual CRISPR-Cas9 system (61), and induced deletions of the lncRNA#32 locus. As BJ cells do not form single clones, generation of monoclonal population of deleted cells was not possible. Instead, we performed a functional genetic experiment to test whether the cells containing the lncRNA#32 deletion are enriched in cells undergoing OIS. Notably, Supplementary Figure S4A shows that control-transduced BJ cells completely senesced, p53 knockout BJ cells strongly bypassed OIS, and targeting lncRNA#32 attenuated senescence, albeit to a lesser extent than p53KO. To confirm that the dual CRISPR-Cas9 system triggered deletion of lncRNA#32, we isolated genomic DNA and performed semi-quantitative PCR to detect lncRNA#32 with oligos (FW: TGGAGGGCTGAATCATCAAGTT, REV: ACTTCAAAGGGCAATTGCTGAAC) surrounding the CRISPR-target region. While wild-type and control-transduced cells produced only one band of about 1.8 Kb, cells transduced with the lncRNA#32-targeting vector showed lncRNA#32 deleted bands (~350 bp), indicating the functionality of the CRISPR vector (Supplementary Figure S4B). Intriguingly, the PCR signal of the deletion band increased after 2 and 3 weeks following OIS induction, in line with a bypass of the OIS phenotype. In comparison, no enrichment of the deleted allele was noted following 3 weeks of culturing without induction of OIS (Supplementary Figure S4B). This indicates that lncRNA#32 deletion gives growth advantage only under OIS conditions. As expected, we found by qRT-PCR that cells expressing sgRNAs targeting lncRNA#32 have reduced level of lncRNA#32 (Supplementary Figure S4C). Sanger sequencing confirmed the correct deletion of lncRNA#32 (Supplementary Figure S4D). For simplicity and in conjunction with its function, we hereafter refer to lncRNA#32 as lncRNA-OIS1.

To extend our finding on the role of lncRNA-OIS1 in OIS we employed a different cell system. We transduced all four functional shRNAs targeting lncRNA-OIS1 (#32–2, 3, 8 and 9, which we renamed KD1, 2, 3 and 4, respectively) into TIG3 cells expressing hTERT and 4-OH-tamoxifen (4-OHT)-inducible oncogenic H-Ras^{V12}, and repeated the BrdU labeling and SA- β -Gal experiments. First, q-RT-PCR and GRO-seq analysis indicated upregulation of lncRNA-OIS1 following oncogenic RAS induction (Supplementary Figures S5E and S9A). Second, as expected, the introduction of all four lncRNA-OIS1 shRNAs reduced lncRNA-OIS1 expression (Supplementary Figure S5E). Last, and

most profoundly, all four lncRNA-OIS1 shRNAs very effectively bypassed OIS as measured by the proliferation and senescent assays BrdU and SA- β -Gal, respectively (Supplementary Figure S5A–D). Altogether, our results demonstrate that intact lncRNA-OIS1 is required for senescence induction following RAS^{V12} activation in primary human cells.

Knockdown of lncRNA-OIS1 abolishes OIS gene expression signature

Next, we sought to explore the mode of action of lncRNA-OIS1 in senescence. To this goal, we first performed RNA-seq of cells transduced with shRNAs against lncRNA-OIS1, the positive controls p53 and BRD7, and negative controls (Figure 3A). Comparison of gene expression profiles in negative controls and p53kd cells upon activation of oncogenic RAS (the former enters senescence while the latter bypasses it) identified 885 differentially expressed genes (386 up- and 499 downregulated in senescent cells) (Figure 3B). Functional enrichment analysis showed that the set of genes whose expression was significantly repressed in senescent cells (compared to the p53kd cells) was markedly enriched for cell-cycle-related genes (Figure 3C), reflecting the strong proliferation arrest that is imposed in negative control cells upon oncogenic stress. This sharp downregulation of cell-cycle genes defines a molecular signature that characterizes the induction of the senescent physiological state. Remarkably, knocking-down lncRNA-OIS1 significantly abolished the repression of these genes (Figure 3D). The effect observed for lncRNA-OIS1-kd was comparable to the effect obtained by BRD7-kd but weaker than the effect elicited by p53-kd (Figure 3D). In accordance with the phenotypic effect of OIS-bypass, we observed that lncRNA-OIS1-kd resulted in attenuation of the induction of CDKN1A (p21), a prime target of p53 that is required for OIS in BJ cells (Supplementary Figure S6A). We confirmed this result at the protein level using western blot analysis (Figure 3E and Supplementary Figure S6B). We included one shRNA (#32–6) which did not give knockdown of lncRNA-OIS1 and showed no bypass of the senescence phenotype (Figure 3E and Supplementary Figure S6B) to demonstrate specificity of the decreased expression of CDKN1A due to lncRNA-OIS1-kd.

To further characterize the effect of knocking-down lncRNA-OIS1 on the cellular transcriptome, we systematically compared, using GSEA analysis (52), gene expression profiles in cells induced for oncogenic RAS and transduced either with shRNAs against lncRNA-OIS1 or with non-targeting shRNAs. As expected from the phenotypic effect and inline with the above analysis, the strongest gene sets that were upregulated upon knocking-down lncRNA-OIS1 were related to proliferation and cell-cycle (Supplementary Figure S6C). A set of genes that are induced in response to ionizing irradiation was the most significantly downregulated gene set in the lncRNA-OIS1 kd cells. This set contains numerous p53 direct target genes, indicating that attenuated expression of lncRNA-OIS1 compromises the activation of the p53 network (Supplementary Figure S6C). In addition, genes of the oxidative phosphorylation pathway are downregulated too in the lncRNA-OIS1 kd cells.

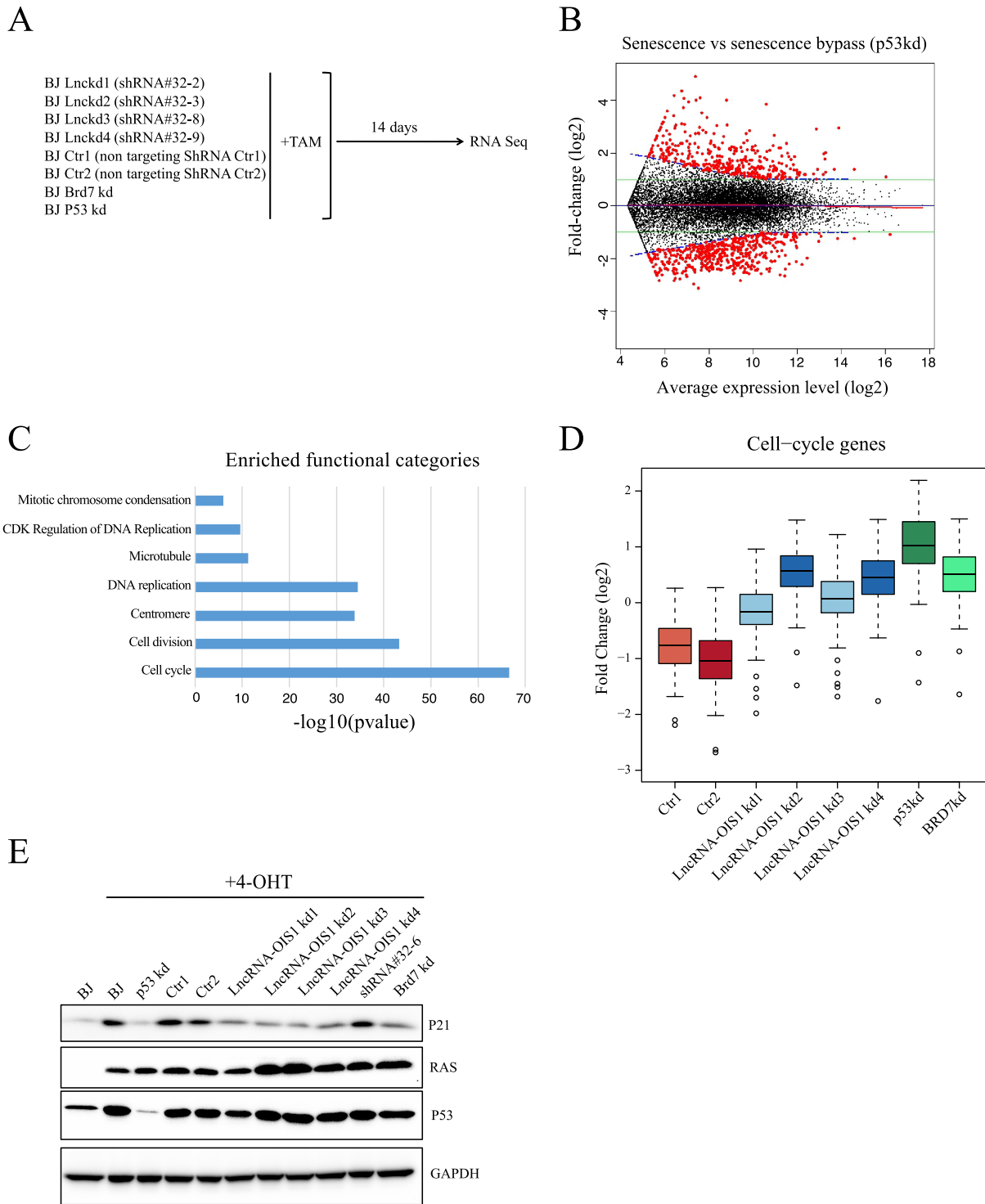


Figure 3. LncRNA-OIS1 knockdown shows a gene expression signature characteristic of senescence bypass. **(A)** A scheme of the RNA-seq experiment. RNA was collected from positive and negative control cells, and the various lncRNA-OIS1kd cells treated with 4-OHT for 14 days. Cells knocked-down for p53 and BRD7 served as positive controls. **(B)** The comparison of gene expression profiles between p53kd and negative control cells, both treated with 4-OHT to induce oncogenic RAS, identified 885 differentially expressed genes. A total of 386 and 499 genes were up- and downregulated, respectively. **(C)** Enriched functional categories in the set of genes that were downregulated in the senescent cells. As expected, the enriched categories are related to cell proliferation and cell division. **(D)** For each of the conditions that we examined, we calculated the distribution of fold-change of expression for the set of 135 cell-cycle genes whose expression is downregulated in senescence, relative to their expression in control untreated cells. In control cells, 4-OHT treatment resulted in strong suppression of this set of genes (Ctrl1, Ctrl2 samples). In contrast, in lncRNA-OIS1-kd cells, the expression of these cell-cycle genes was elevated compared to control cells. Notably, the effect observed in lncRNA-OIS1kds was similar to the effect of BRD7, but, as expected, weaker than that of the p53kd. **(E)** CDKN1A protein levels examined by western blotting.

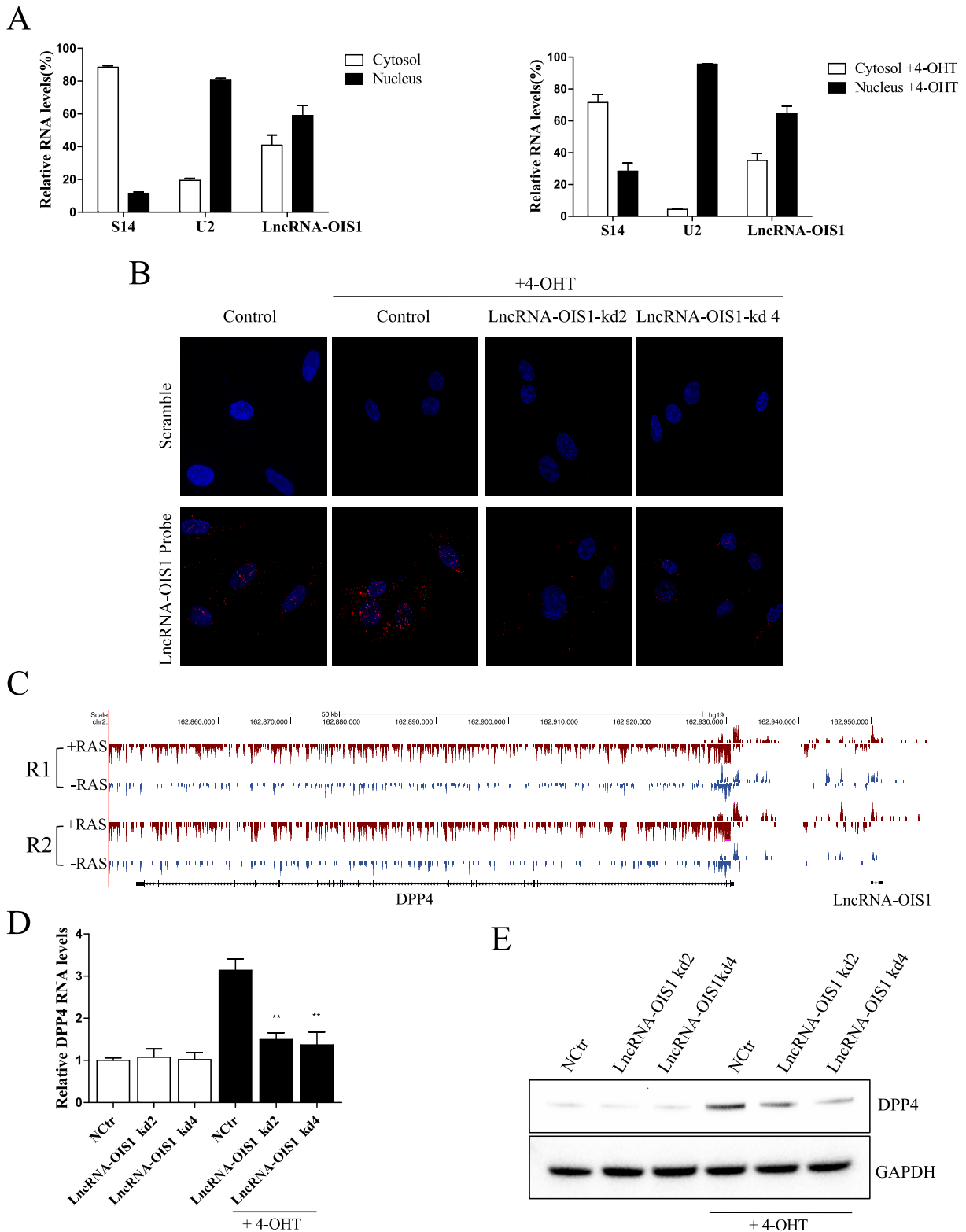


Figure 4. LncRNA-OIS1 expression is required for the activation of DPP4 in response to oncogenic stress. **(A)** Subcellular localization of LncRNA-OIS1 in BJ cells treated with or without 4-OHT. U2 and S14 RNAs were used as controls for nucleus and cytosol fractions, respectively. **(B)** ISH of LncRNA-OIS1 in BJ cells treated with or without 4-OHT. **(C)** Screenshots of GRO-seq data of the LncRNA-OIS1 and DPP4 genomic locus. R1 and R2 are two biological replicates. **(D)** qRT-PCR analysis of DPP4 expression upon LncRNA-OIS1kd treated with or without 4-OHT, $**P < 0.002$, two-tailed Student's *t*-test. **(E)** DPP4 protein levels examined by western blotting.

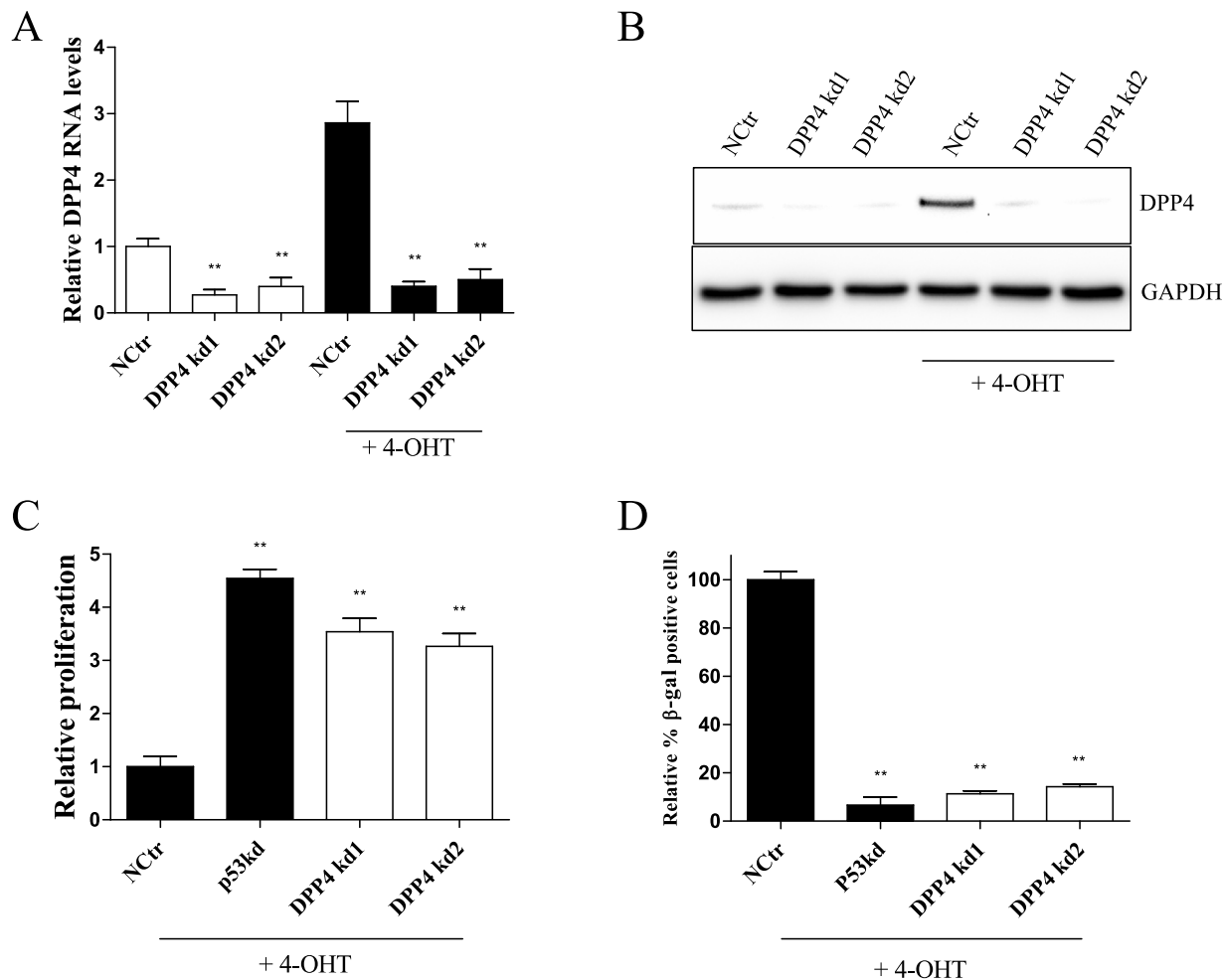


Figure 5. Induction of DPP4 is required for OIS. (A) qRT-PCR analysis of DPP4 expression upon DPP4kd (two different shRNAs) treated with or without 4-OHT, $**P < 0.005$, two-tailed Student's *t*-test. (B) Western blot analysis of DPP4 protein. (C) BrdU proliferation analysis of DPP4kd BJ-RAS^{V12} cells, $**P < 0.0005$, two-tailed Student's *t*-test. The percentage of BrdU-positive cells was normalized to negative control cells. (D) Senescence SA-β-Gal assay. $**P < 0.0005$, two-tailed Student's *t*-test. The percentage of β-gal-positive cells was normalized to negative control cells.

Notably, all these gene sets show the opposite response in cells that enter senescence in response to oncogenic stress (Supplementary Figure S6C), demonstrating that loss of lncRNA-OIS1 abolishes OIS gene expression signature.

Loss-of lncRNA-OIS1 compromises the induction of DPP4 by OIS

To investigate the mechanism(s) by which lncRNA-OIS1 affects OIS induction, we first examined its subcellular localization. In control BJ/ET/Ras^{V12}ER cells, lncRNA-OIS1 was located both in the nucleus and the cytosol. Following RAS^{V12} activation, lncRNA-OIS1 maintained a similar pattern in these two compartments (Figure 4A). ISH analysis confirmed lncRNA-OIS1 increased expression following RAS^{V12} induction, and its localization in the nucleus and cytosol. Loss-of lncRNA-OIS1 confirmed the specificity of the signal to lncRNA-OIS1 (Figure 4B).

lncRNAs can impact the expression of nearby genes on the chromatin (*cis* function), or affect gene expression in trans (for example by controlling mRNA transcription, splicing and translation). We therefore first in-

terrogated whether lncRNA-OIS1 functions *in trans*, and whether ectopic expression of lncRNA-OIS1 can drive cells into senescence without RAS induction. We over-expressed lncRNA-OIS1 in primary BJ cells (full length or exons; Supplementary Figure S7A), but observed no induction of senescence as measured by BrdU labeling and SA-β-Gal assays (Supplementary Figure S7B–D). Second, we over-expressed lncRNA-OIS1 (both full length and exons) in lncRNA-OIS1-kd cells to test whether ectopic expression of lncRNA-OIS1 can restore the senescence phenotype. However, despite the high expression of lncRNA-OIS1 (Supplementary Figure S8A), OIS-bypass by lncRNA-OIS1-kd was maintained (Supplementary Figure S8B–D). These data indicated that lncRNA-OIS1 does not function in trans, rather, a localized expression and effect on neighboring genes is required (*cis* effect).

In general, lncRNAs can be physically linked to the locus from which they are encoded, and exert its function during transcription without the need for processing or shuttling. Well-studied examples of *cis*-acting lncRNAs are those that cause X-inactivation (62,63). Examples of other

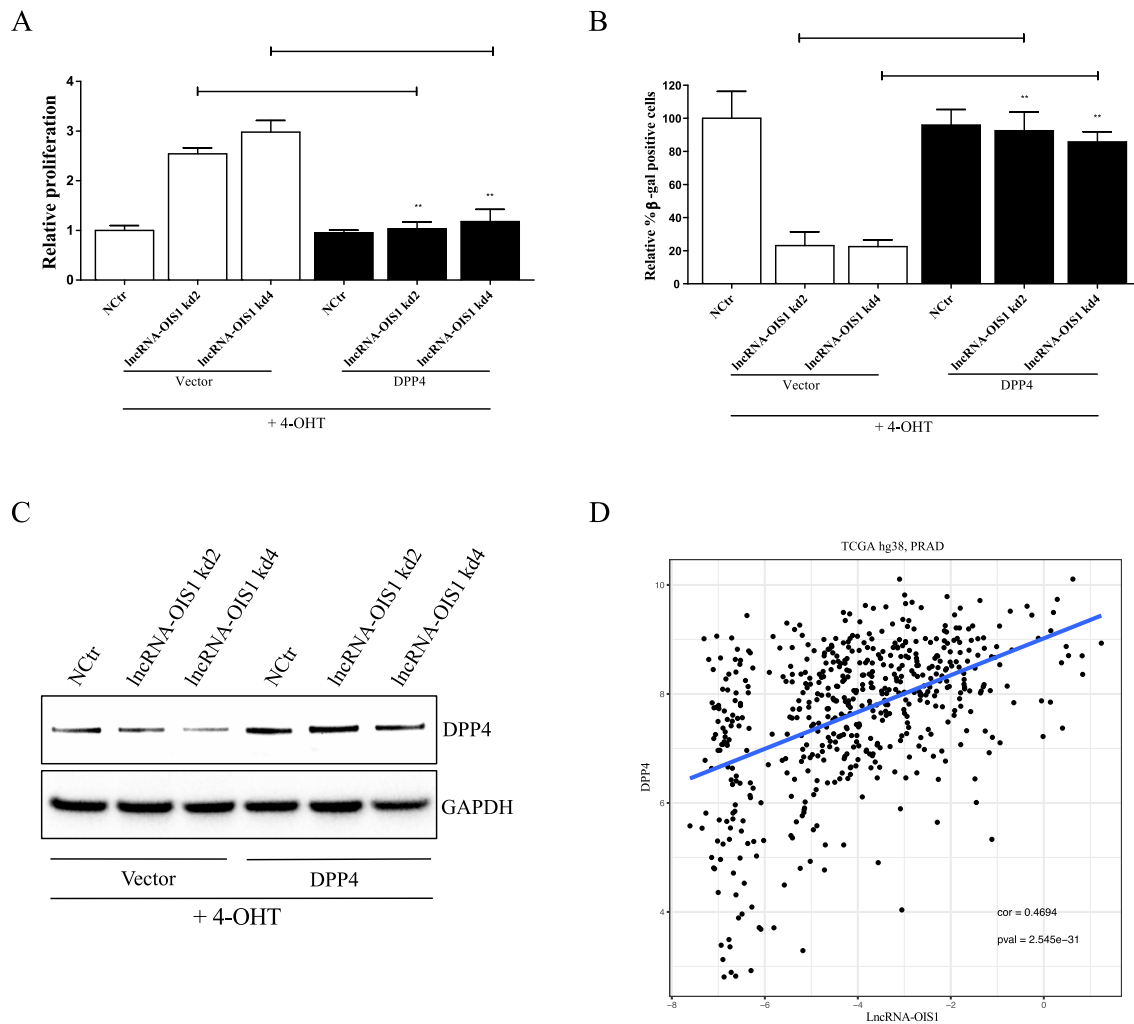


Figure 6. Ectopic expression of DPP4 induces senescence in lncRNA-OIS1kd cells. **(A)** BrdU proliferation assay of DPP4 or vector-transduced BJ-RAS^{V12}-lncRNA-OIS1kd cells. ****P** < 0.001, two-tailed Student's *t*-test. The percentage of BrdU-positive cells was normalized to negative control cells. **(B)** SA-β-Gal assay. ****P** < 0.001, two-tailed Student's *t*-test. The percentage of β-gal-positive cells was normalized to negative control cells. **(C)** Western blot analysis of DPP4 protein. **(D)** TCGA data analysis of lncRNA-OIS1 and DPP4 expression in PRAD samples ($r = 0.469$, P -value = $2.5e^{-31}$).

cis-regulatory lncRNAs include ncRNA-a1–7, Hottip and Mistral, the perturbation of which lead to decreased expression of nearby genes (64–67), suggesting that gene regulation in *cis* is a very important mode of lncRNA action. To investigate whether lncRNA-OIS1 expression influences nearby genes, we analyzed Global Run-On Sequencing data (GRO-Seq) of senescent and proliferation BJ cells (55). We observed that both lncRNA-OIS1 and its nearby gene DPP4 were increased in the BJ cells upon RAS induction (Figure 4C). We also observed the same effect in TIG3 cells (Supplementary Figure S9A). Additionally, loss-of lncRNA-OIS1 abolished the activation of DPP4 following oncogene induction based on BJ cells RNA-seq data (Supplementary Figure S9B). We solidified these results by qRT-PCR (Figure 4D and Supplementary Figure S9C) and chose the best two lncRNA-OIS1 knockdowns (KD2 and 4) for western blot analyses of DPP4 expression four days following RAS^{V12} induction, before the cell-cycle is arrested and senescence is established (Figure 4D and E). Indeed, attenuated activation of DPP4 protein expression was ob-

tained in cells with lncRNA-OIS knockdown. A similar effect was also observed in TIG3 lncRNA-OIS1-kd cells 4 days following RAS^{V12} induction (Supplementary Figure S9D). Altogether, these data link lncRNA-OIS1 to regulation of DPP4 expression and to the senescent phenotype induced by oncogenic RAS.

Loss-of DPP4 bypasses OIS

Interestingly, it has been reported that DPP4 is a tumor suppressor in melanoma (68,69), non-small cell lung cancer (70), ovarian cancer (71–73), endometrial carcinoma (74), prostate cancer (75), neuroblastoma (76) and glioma (77). We therefore hypothesized that the tumor suppressive role of DPP4 is linked to OIS. To examine this issue, we generated shRNAs (Supplementary Table S7) transduced DPP4 knockdown BJ cells. qRT-PCR and western blot analyses confirmed significant reduction of DPP4 mRNA and protein levels upon knockdown (Figure 5A and B). As predicted, loss-of DPP4 bypassed OIS, as determined by pro-

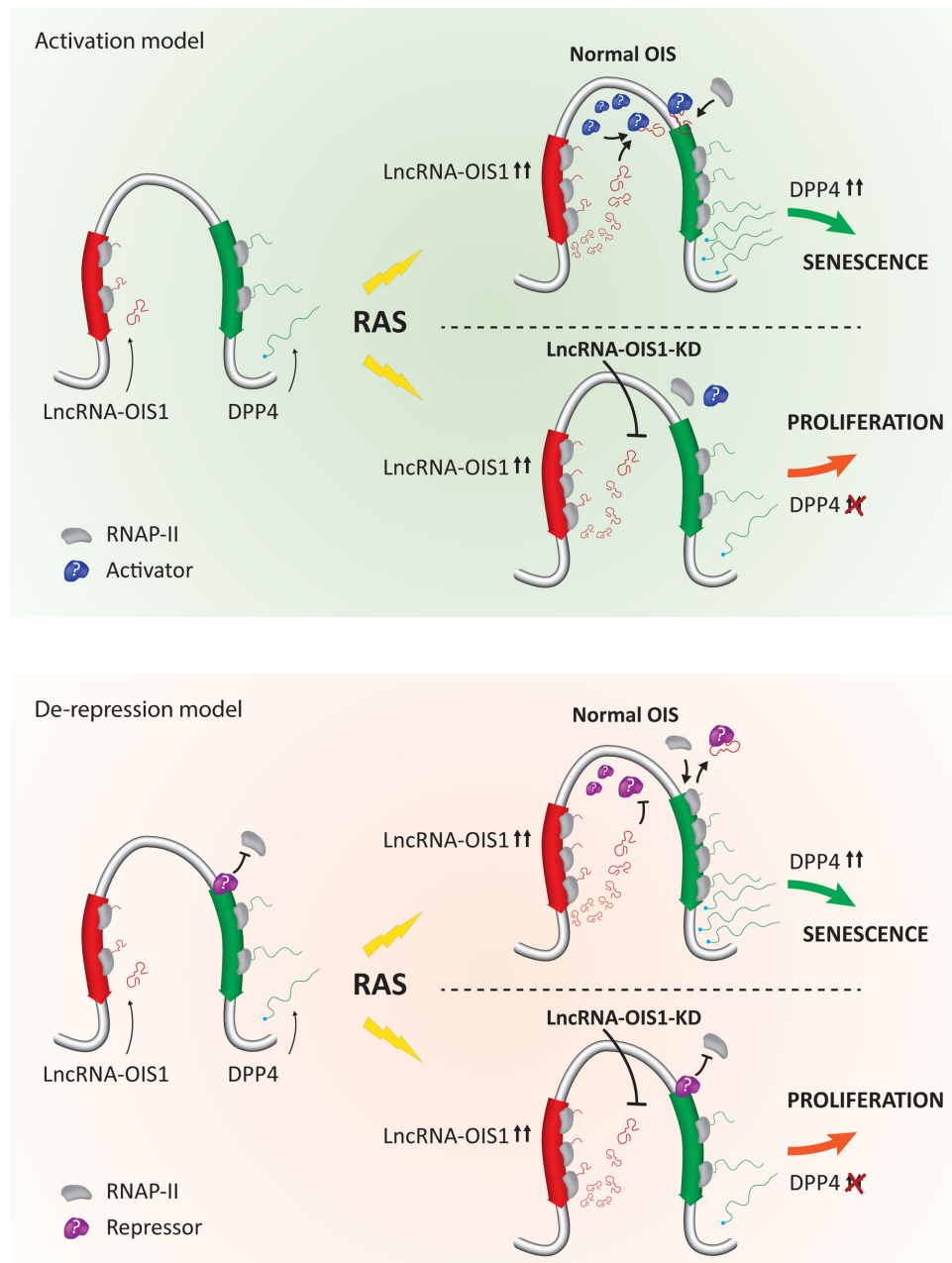


Figure 7. Schematic representation of lncRNA-OIS1 function in normal and senescence conditions.

liferation and SA- β -Gal assays (Figure 5C and D; Supplementary Figure S9E). Next, we examined whether lncRNA-OIS1 regulates senescence through DPP4. We cloned DPP4 in a lentiviral vector, ectopically expressed it in lncRNA-OIS1-kd cells and induced OIS. Intriguingly, proliferation (BrdU labeling) and SA- β -Gal assays demonstrated that ectopic expression of DPP4 abolished the senescence bypass phenotype of lncRNA-OIS1-kd cells, while a control vector did not (Figure 6A and B; Supplementary Figure S10A and B). We confirmed the overexpression of DPP4 by western blot (Figure 6C and Supplementary Figure S10C). These experiments indicate that DPP4 is the relevant target gene

of lncRNA-OIS1 during OIS, and that lncRNA-OIS1 is a major determinant of DPP4 function in OIS.

Association of lncRNA-OIS1 and DPP4 in the tumors

Last, we interrogated lncRNA-OIS1 expression in tumors and its correlation with that of DPP4 by analyzing TCGA data. lncRNA-OIS1 is very lowly expressed in most tumor types (Supplementary Figure S11A). We plotted the read counts of the lncRNA-OIS1 among normal and tumor samples, indicating in each type the number of samples with at least one read count for lncRNA-OIS1. Interestingly, prostate adenocarcinoma (PRAD) samples showed clear lncRNA-OIS1 expression. Using this dataset for dif-

ferential expression analysis, we observed no change between tumor and normal samples (empirical Bayes test, $B = -5.79$, P -value = 0.28) (Supplementary Table S4), but a significant positive correlation between lncRNA-OIS1 and DPP4 expression in the tumor samples ($r = 0.469$, P -value = $2.5e^{-31}$) (Figure 6D), suggesting that at least in PRAD DPP4 expression is controlled by lncRNA-OIS1.

DISCUSSION

Over the past few years, numerous lncRNAs have been discovered and characterized as critical factors in physiological and pathological processes. However, the role of lncRNAs in OIS remained unexplored. Here, we contribute to the understanding of the function of lncRNAs by describing a role of lncRNA-OIS1 in cellular senescence provoked by the expression of oncogenic RAS (OIS). Upregulation of lncRNA-OIS1 following OIS was required for the induction of DPP4, a well-described gene with tumor suppressive activity. Differential gene expression analyses of lncRNA-OIS1 knockdown cells indicated attenuated activation of CDKN1A following OIS induction, and confirmed changes in cell-cycle regulatory genes favoring cellular proliferation. Gene complementation experiments indicated that DPP4, a lncRNA-OIS1 neighboring gene, is the downstream target of lncRNA-OIS1 in senescence. Exactly how DPP4 affects CDKN1A and cell-cycle genes, and how lncRNA-OIS1 controls DPP4 expression, remains to be uncovered. Nevertheless, we describe here an important function of lncRNAs with potentially influential implications in cancer biology.

OIS is a major senescence type and it poses a critical barrier to cancer. A recent study has shown that the lncRNA-MIR31HG was a senescence modulator during BRAF-V600 induced senescence in TIG3 cells (46). It has also been shown that loss-of MIR31HG reduces cell growth and promotes a strong senescence phenotype through the regulation of the tumor suppressor P16^{INK4A}. Here, we add to this knowledge by identifying and characterizing the role of lncRNA-OIS1 in regulating senescence through the control of a nearby gene DPP4.

Interestingly, we also overexpressed lncRNA-OIS1 in BJ cells to examine whether high levels of the lncRNA-OIS1 can drive cells into senescence. However, we neither observed senescence induction nor DPP4 was activated (Supplementary Figure S7). Additionally, also the ectopic expression of lncRNA-OIS1 was not able to revert the bypass of senescence and the reduced DPP4 activation induced by lncRNA-OIS1 knockdown under OIS (Supplementary Figure S8). This is indicative of a cis function of lncRNA-OIS1. Indeed, we identified DPP4, a nearby gene to lncRNA-OIS1, as a key component of OIS. First, loss-of DPP4, similar to lncRNA-OIS1 loss, resulted in bypass of senescence (Figure 5). Second, ectopic expression of DPP4 reverted the bypass of senescence induced by the loss-of lncRNA-OIS1 (Figure 6A–C and Supplementary Figure S10). Additionally, a recent research found that DPP4 can regulate senescence in WI-38 cells, strongly supporting our observations (78). However, although both lncRNA-OIS1 and DPP4 genes reside in the same topologically associating chromatin domain through a CCCTC-binding factor (CTCF) loop

(Supplementary Figure S12A), and chromatin loops can be identified in various ChIA-PET and Hi-C chromatin conformation capture datasets (Supplementary Figure S12B), we did not observe a clear direct interaction of lncRNA-OIS1 locus with the promoter of DPP4 using 4C, a chromatin capture analysis technique, through two distinct view point sites (Supplementary Figure S13A). Thus, how exactly the expression of DPP4 depends on lncRNA-OIS1 remains unclear. We speculate that lncRNA-OIS1 expression may be required to allow high chromatin accessibility to senescence-associated DPP4-activating transcription factors by directly recruiting essential transcription factors, or alternatively by counteracting chromatin-repressive components of the chromatin (Figure 7). Nevertheless, our findings here elucidate the importance of lncRNA-OIS1 for eliciting a proper cellular response to the emergence of oncogenic stress.

DATA AVAILABILITY

RNA-seq, Ribosome profiling (Ribo-seq), GRO-seq data are deposited in GEO DB (accession number GSE42509, GSE106414, GSE109290).

SUPPLEMENTARY DATA

Supplementary Data are available at NAR Online.

ACKNOWLEDGEMENTS

We thank the China Scholarship Council for support. RNA Train supports our research and provides a great platform for training, learning, calibration. We thank all the members of the Agami group for helpful discussions. We thank Andrea Ventura for kindly providing the plasmid PX333 and all the reagents for lncRNA-OIS1 deletion. We also want to thank Jing Li (Cnkingbio Company) for helpful suggestions.

FUNDING

This work was supported by the China Scholarship Council (CSC) (to L.L.); ERC-AdG enhReg [322493 to R.A.]; ERC-ITN RNA TRAIN [607720 to R.A.]; Edmond J. Safra Center for Bioinformatics Fellowship (to R.E.). The Human Frontier Science Program [LT000640/2013 to Alejandro Pineiro Ugalde]. Funding for open access charge: CSC; ERC-AdG enhReg [322493]; RNA Train [607720].

Conflict of interest statement. None declared.

REFERENCES

- Cabili, M., Trapnell, C., Goff, L., Koziol, M., Tazon-Vega, B., Regev, A. and Rinn, J.L. (2011) Integrative annotation of human large intergenic noncoding RNAs reveals global properties and specific subclasses. *Genes Dev.*, **25**, 1915–1927.
- Djebali, S., Davis, C.A., Merkel, A., Dobin, A., Lassmann, T., Mortazavi, A., Tanzer, A., Lagarde, J., Lin, W., Schlesinger, F. *et al.* (2012) Landscape of transcription in human cells. *Nature*, **489**, 101–108.
- Guttman, M., Russell, P., Ingolia, N.T., Weissman, J.S. and Lander, E.S. (2013) Ribosome profiling provides evidence that large noncoding RNAs do not encode proteins. *Cell*, **154**, 240–251.

4. Guttman, M., Amit, I., Garber, M., French, C., Lin, M.F., Feldser, D., Huarte, M., Zuk, O., Carey, B.W., Cassady, J.P. *et al.* (2009) Chromatin signature reveals over a thousand highly conserved large non-coding RNAs in mammals. *Nature*, **458**, 223–227.
5. Guttman, M., Donaghey, J., Carey, B.W., Garber, M., Grenier, J.K., Munson, G., Young, G., Lucas, A.B., Ach, R., Bruhn, L. *et al.* (2011) lincRNAs act in the circuitry controlling pluripotency and differentiation. *Nature*, **477**, 295–300.
6. Wapinski, O. and Chang, H.Y. (2011) Long noncoding RNAs and human disease. *Trends Cell Biol.*, **21**, 354–361.
7. Tsai, M.C., Spitale, R.C. and Chang, H.Y. (2011) Long intergenic noncoding RNAs: New links in cancer progression. *Cancer Res.*, **71**, 3–7.
8. Batista, P.J. and Chang, H.Y. (2013) Long noncoding RNAs: cellular address codes in development and disease. *Cell*, **152**, 1298–1307.
9. Qureshi, I.A. and Mehler, M.F. (2012) Emerging roles of non-coding RNAs in brain evolution, development, plasticity and disease. *Nat. Rev. Neurosci.*, **13**, 528–541.
10. Ghosal, S., Das, S. and Chakrabarti, J. (2013) Long noncoding RNAs: new players in the molecular mechanism for maintenance and differentiation of pluripotent stem cells. *Stem Cells Dev.*, **22**, 2240–2253.
11. Lee, J.T. (2012) Epigenetic regulation by long noncoding RNAs. *Science*, **338**, 1435–1439.
12. Gong, C. and Maquat, L.E. (2011) lncRNAs transactivate STAU1-mediated mRNA decay by duplexing with 3' UTRs via Alu elements. *Nature*, **470**, 284–288.
13. Yoon, J.-H., Abdelmohsen, K. and Gorospe, M. (2013) Posttranscriptional gene regulation by long noncoding RNA. *J. Mol. Biol.*, **425**, 3723–3730.
14. Cesana, M., Cacchiarelli, D., Legnini, I., Santini, T., Sthandier, O., Chinappi, M., Tramontano, A. and Bozzoni, I. (2011) A long noncoding RNA controls muscle differentiation by functioning as a competing endogenous RNA. *Cell*, **147**, 358–369.
15. Bergmann, J.H. and Spector, D.L. (2014) Long non-coding RNAs: Modulators of nuclear structure and function. *Curr. Opin. Cell Biol.*, **26**, 10–18.
16. Petruk, S., Sedkov, Y., Riley, K.M., Hodgson, J., Schweisguth, F., Hirose, S., Jaynes, J.B., Brock, H.W. and Mazo, A. (2006) Transcription of bxd noncoding RNAs promoted by trithorax represses Ubx in cis by transcriptional interference. *Cell*, **127**, 1209–1221.
17. Zhao, J., Sun, B.K., Erwin, J.A., Song, J.-J. and Lee, J.T. (2008) Polycomb proteins targeted by a short repeat RNA to the mouse X chromosome. *Science*, **322**, 750–756.
18. Melo, C.A., Drost, J., Wijchers, P.J., van de Werken, H., de Wit, E., Vrieling, J.A.F.O., Elkon, R., Melo, S.A., Léveillé, N., Kalluri, R. *et al.* (2013) ERNAs are required for p53-dependent enhancer activity and gene transcription. *Mol. Cell*, **49**, 524–535.
19. Gupta, R.A., Shah, N., Wang, K.C., Kim, J., Horlings, H.M., Wong, D.J., Tsai, M.-C., Hung, T., Argani, P., Rinn, J.L. *et al.* (2010) Long non-coding RNA HOTAIR reprograms chromatin state to promote cancer metastasis. *Nature*, **464**, 1071–1076.
20. Tsai, M.-C., Manor, O., Wan, Y., Mosammammarast, N., Wang, J.K., Lan, F., Shi, Y., Segal, E. and Chang, H.Y. (2010) Long noncoding RNA as modular scaffold of histone modification complexes. *Science*, **329**, 689–693.
21. Huarte, M., Guttman, M., Feldser, D., Garber, M., Koziol, M.J., Kenzelmann-Broz, D., Khalil, A.M., Zuk, O., Amit, I., Rabani, M. *et al.* (2010) A large intergenic noncoding RNA induced by p53 mediates global gene repression in the p53 response. *Cell*, **142**, 409–419.
22. Ulitsky, I. and Bartel, D.P. (2013) lincRNAs: genomics, evolution, and mechanisms. *Cell*, **154**, 26–46.
23. Kornienko, A.E., Guenzl, P.M., Barlow, D.P. and Pauler, F.M. (2013) Gene regulation by the act of long non-coding RNA transcription. *BMC Biol.*, **11**, 59.
24. Hayflick, L. (1965) The limited in vitro lifetime of human diploid cell strains. *Exp. Cell Res.*, **37**, 614–636.
25. Kuilman, T., Michaloglou, C., Mooi, W.J. and Peeper, D.S. (2010) The essence of senescence. *Genes Dev.*, **24**, 2463–2479.
26. Serrano, M., Lin, A.W., McCurrach, M.E., Beach, D. and Lowe, S.W. (1997) Oncogenic ras provokes premature cell senescence associated with accumulation of p53 and p16(INK4a). *Cell*, **88**, 593–602.
27. Campisi, J. (2005) Senescent cells, tumor suppression, and organismal aging: Good citizens, bad neighbors. *Cell*, **120**, 513–522.
28. Baker, D.J., Wijshake, T., Tchikonia, T., LeBrasseur, N.K., Childs, B.G., van de Sluis, B., Kirkland, J.L. and van Deursen, J.M. (2011) Clearance of p16Ink4a-positive senescent cells delays ageing-associated disorders. *Nature*, **479**, 232–236.
29. Kuilman, T., Michaloglou, C., Vredeveld, L.C.W., Douma, S., van Doorn, R., Desmet, C.J., Aarden, L.A., Mooi, W.J. and Peeper, D.S. (2008) Oncogene-induced senescence relayed by an interleukin-dependent inflammatory network. *Cell*, **133**, 1019–1031.
30. Freund, A., Orjalo, A.V., Desprez, P.Y. and Campisi, J. (2010) Inflammatory networks during cellular senescence: causes and consequences. *Trends Mol. Med.*, **16**, 238–246.
31. Gorospe, M. and Abdelmohsen, K. (2011) MicroRegulators come of age in senescence. *Trends Genet.*, **27**, 233–241.
32. Luo, X.-G., Ding, J.-Q. and Chen, S.-D. (2010) Microglia in the aging brain: relevance to neurodegeneration. *Mol. Neurodegener.*, **5**, 12.
33. Ohtani, N., Takahashi, A., Mann, D.J. and Hara, E. (2012) Cellular senescence: a double-edged sword in the fight against cancer. *Exp. Dermatol.*, **21**(Suppl. 1), 1–4.
34. Krtolica, A., Parrinello, S., Lockett, S., Desprez, P.-Y. and Campisi, J. (2001) Senescent fibroblasts promote epithelial cell growth and tumorigenesis: a link between cancer and aging. *Proc. Natl. Acad. Sci. U.S.A.*, **98**, 12072–12077.
35. Salama, R., Sadaie, M., Hoare, M. and Narita, M. (2014) Cellular senescence and its effector programs. *Genes Dev.*, **28**, 99–114.
36. Coppé, J.-P., Desprez, P.-Y., Krtolica, A. and Campisi, J. (2010) The senescence-associated secretory phenotype: the dark side of tumor suppression. *Annu. Rev. Pathol. Mech. Dis.*, **5**, 99–118.
37. Rodier, F. and Campisi, J. (2011) Four faces of cellular senescence. *J. Cell Biol.*, **192**, 547–556.
38. Collado, M., Blasco, M.A. and Serrano, M. (2007) Cellular senescence in cancer and aging. *Cell*, **130**, 223–233.
39. Campisi, J. (2003) Cancer and ageing: rival demons? *Nat. Rev. Cancer*, **3**, 339–349.
40. Lanigan, F., Geraghty, J.G. and Bracken, A.P. (2011) Transcriptional regulation of cellular senescence. *Oncogene*, **30**, 2901–2911.
41. Wang, W., Yang, X., Cristofalo, V.J., Holbrook, N.J. and Gorospe, M. (2001) Loss of HuR is linked to reduced expression of proliferative genes during replicative senescence. *Mol. Cell Biol.*, **21**, 5889–5898.
42. Pont, A.R., Sadri, N., Hsiao, S.J., Smith, S. and Schneider, R.J. (2012) mRNA decay factor AUF1 maintains normal aging, telomere maintenance, and suppression of senescence by activation of telomerase transcription. *Mol. Cell*, **47**, 5–15.
43. Sanduja, S., Kaza, V. and Dixon, D.A. (2009) The mRNA decay factor tristetraprolin (TTP) induces senescence in human papillomavirus-transformed cervical cancer cells by targeting E6-AP ubiquitin ligase. *Aging (Albany NY)*, **1**, 803–817.
44. Xie, H.-F., Liu, Y.-Z., Du, R., Wang, B., Chen, M.-T., Zhang, Y.-Y., Deng, Z.-L. and Li, J. (2017) miR-377 induces senescence in human skin fibroblasts by targeting DNA methyltransferase 1. *Cell Death Dis.*, **8**, e2663.
45. Xu, D., Takeshita, F., Hino, Y., Fukunaga, S., Kudo, Y., Tamaki, A., Matsunaga, J., Takahashi, R. u., Takata, T., Shimamoto, A. *et al.* (2011) miR-22 represses cancer progression by inducing cellular senescence. *J. Cell Biol.*, **193**, 409–424.
46. Montes, M., Nielsen, M.M., Maglieri, G., Jacobsen, A., Højfeldt, J., Agrawal-Singh, S., Hansen, K., Helin, K., van de Werken, H.J.G., Pedersen, J.S. *et al.* (2015) The lncRNA MIR31HG regulates p16(INK4A) expression to modulate senescence. *Nat. Commun.*, **6**, 6967.
47. Wu, C.L., Wang, Y., Jin, B., Chen, H., Xie, B.S. and Mao, Z.B. (2015) Senescence-associated long non-coding RNA (SALNR) delays oncogene-induced senescence through NF90 regulation. *J. Biol. Chem.*, **290**, 30175–30192.
48. Drost, J., Mantovani, F., Tocco, F., Elkon, R., Comel, A., Holstege, H., Kerkhoven, R., Jonkers, J., Voorhoeve, P.M., Agami, R. *et al.* (2010) BRD7 is a candidate tumour suppressor gene required for p53 function. *Nat. Cell Biol.*, **12**, 380–389.
49. Kim, D., Perte, G., Trapnell, C., Pimentel, H., Kelley, R. and Salzberg, S.L. (2013) TopHat2: accurate alignment of transcriptomes in the presence of insertions, deletions and gene fusions. *Genome Biol.*, **14**, R36.
50. Anders, S., Pyl, P.T. and Huber, W. (2015) HTSeq—a python framework to work with high-throughput sequencing data. *Bioinformatics*, **31**, 166–169.

51. Huang, D.W., Sherman, B.T. and Lempicki, R.A. (2008) Systematic and integrative analysis of large gene lists using DAVID bioinformatics resources. *Nat. Protoc.*, **4**, 44–57.
52. Subramanian, A., Tamayo, P., Mootha, V.K., Mukherjee, S., Ebert, B.L., Gillette, M.A., Paulovich, A., Pomeroy, S.L., Golub, T.R., Lander, E.S. *et al.* (2005) Gene set enrichment analysis: a knowledge-based approach for interpreting genome-wide expression profiles. *PNAS*, **102**, 15545–15550.
53. Soares, R.J., Maglieri, G., Gutschner, T., Diederichs, S., Lund, A.H., Nielsen, B.S. and Holmström, K. (2018) Evaluation of fluorescence in situ hybridization techniques to study long non-coding RNA expression in cultured cells. *Nucleic Acids Res.*, **46**, e4.
54. Loayza-Puch, F., Rooijers, K., Buil, L.C.M., Zijlstra, J.F., Oude Vrielink, J., Lopes, R., Ugalde, A.P., van Breugel, P., Hofland, I., Wesseling, J. *et al.* (2016) Tumour-specific proline vulnerability uncovered by differential ribosome codon reading. *Nature*, **530**, 490–494.
55. Korkmaz, G., Lopes, R., Ugalde, A.P., Nevedomskaya, E., Han, R., Myacheva, K., Zwart, W., Elkon, R. and Agami, R. (2016) Functional genetic screens for enhancer elements in the human genome using CRISPR-Cas9. *Nat. Biotechnol.*, **34**, 1–10.
56. Agami, R. and Bernard, R. (2000) Distinct initiation and maintenance mechanisms cooperate to induce G1 cell cycle arrest in response to DNA damage. *Cell*, **102**, 55–66.
57. Haarhuis, J.H.I., van der Weide, R.H., Blomen, V.A., Yáñez-Cuna, J.O., Amendola, M., van Ruiten, M.S., Krijger, P.H.L., Teunissen, H., Medema, R.H., van Steensel, B. *et al.* (2017) The cohesin release factor WAPL restricts chromatin loop extension. *Cell*, **169**, 693–707.
58. van de Werken, H.J.G., Landan, G., Holwerda, S.J.B., Hoichman, M., Klous, P., Chachik, R., Splinter, E., Valdes-Quezada, C., Öz, Y., Bouwman, B.A.M. *et al.* (2012) Robust 4C-seq data analysis to screen for regulatory DNA interactions. *Nat. Methods*, **9**, 969–972.
59. Smyth, G.K. (2005) Limma: linear models for microarray data. In: Gentleman, R., Carey, V., Dudoit, S., Irizarry, R. and Huber, W. (eds). *Bioinformatics and Computational Biology Solutions Using R and Bioconductor*. Springer, NY, pp. 397–420.
60. Law, C.W., Chen, Y., Shi, W. and Smyth, G.K. (2014) voom: precision weights unlock linear model analysis tools for RNA-seq read counts. *Genome Biol.*, **15**, R29.
61. Vidigal, J.A. and Ventura, A. (2015) Rapid and efficient one-step generation of paired gRNA CRISPR-Cas9 libraries. *Nat. Commun.*, **6**, 8083.
62. Lee, J.T. (2009) Lessons from X-chromosome inactivation: Long ncRNA as guides and tethers to the epigenome. *Genes Dev.*, **23**, 1831–1842.
63. Augui, S., Nora, E.P. and Heard, E. (2011) Regulation of X-chromosome inactivation by the X-inactivation centre. *Nat. Rev. Genet.*, **12**, 429–442.
64. Ørom, U.A., Derrien, T., Beringer, M., Gumireddy, K., Gardini, A., Bussotti, G., Lai, F., Zytnicki, M., Notredame, C., Huang, Q. *et al.* (2010) Long noncoding RNAs with enhancer-like function in human cells. *Cell*, **143**, 46–58.
65. Bertani, S., Sauer, S., Bolotin, E. and Sauer, F. (2011) The noncoding RNA mistral activates Hoxa6 and Hoxa7 expression and stem cell differentiation by recruiting MLL1 to chromatin. *Mol. Cell*, **43**, 1040–1046.
66. Wang, K.C., Yang, Y.W., Liu, B., Sanyal, A., Corces-Zimmerman, R., Chen, Y., Lajoie, B.R., Protacio, A., Flynn, R.A., Gupta, R.A. *et al.* (2011) A long noncoding RNA maintains active chromatin to coordinate homeotic gene expression. *Nature*, **472**, 120–124.
67. Lai, F., Orom, U.A., Cesaroni, M., Beringer, M., Taatjes, D.J., Blobel, G.A. and Shiekhattar, R. (2013) Activating RNAs associate with Mediator to enhance chromatin architecture and transcription. *Nature*, **494**, 497–501.
68. Wesley, U.V., Albino, A.P., Tiwari, S. and Houghton, A.N. (1999) A role for dipeptidyl peptidase IV in suppressing the malignant phenotype of melanocytic cells. *J. Exp. Med.*, **190**, 311–322.
69. Pethiyagoda, C.L., Welch, D.R. and Fleming, T.P. (2000) Dipeptidyl peptidase IV (DPP-IV) inhibits cellular invasion of melanoma cells. *Clin. Exp. Metastasis*, **18**, 391–400.
70. Wesley, U.V., Tiwari, S. and Houghton, A.N. (2004) Role for dipeptidyl peptidase IV in tumor suppression of human non small cell lung carcinoma cells. *Int. J. Cancer*, **109**, 855–866.
71. Kajiyama, H., Kikkawa, F., Suzuki, T., Shibata, K., Ino, K. and Mizutani, S. (2002) Prolonged survival and decreased invasive activity attributable to dipeptidyl peptidase IV overexpression in ovarian carcinoma. *Cancer Res.*, **62**, 2753–2757.
72. Kajiyama, H., Kikkawa, F., Khin, E.E., Shibata, K., Ino, K. and Mizutani, S. (2003) Dipeptidyl peptidase IV overexpression induces up-regulation of E-cadherin and tissue inhibitors of matrix metalloproteinases, resulting in decreased invasive potential in ovarian carcinoma cells. *Cancer Res.*, **63**, 2278–2283.
73. Kikkawa, F., Kajiyama, H., Ino, K., Shibata, K. and Mizutani, S. (2003) Increased adhesion potency of ovarian carcinoma cells to mesothelial cells by overexpression of dipeptidyl peptidase IV. *Int. J. Cancer*, **105**, 779–783.
74. Mizokami, Y., Kajiyama, H., Shibata, K., Ino, K., Kikkawa, F. and Mizutani, S. (2004) Stromal cell-derived factor-1 α -induced cell proliferation and its possible regulation by CD26/dipeptidyl peptidase IV in endometrial adenocarcinoma. *Int. J. Cancer*, **110**, 652–659.
75. Wesley, U.V., McGroarty, M. and Homoyouni, A. (2005) Dipeptidyl peptidase inhibits malignant phenotype of prostate cancer cells by regulating basic fibroblast growth factor signaling pathway. *Cancer Res.*, **65**, 1325–1334.
76. Arscott, W.T., LaBauve, A.E., May, V. and Wesley, U.V. (2009) Suppression of neuroblastoma growth by dipeptidyl peptidase IV: relevance of chemokine regulation and caspase activation. *Oncogene*, **28**, 479–491.
77. Busek, P., Stremenova, J., Sromova, L., Hilser, M., Balaziova, E., Kosek, D., Trylcova, J., Strnad, H., Krepela, E. and Sedo, A. (2012) Dipeptidyl peptidase-IV inhibits glioma cell growth independent of its enzymatic activity. *Int. J. Biochem. Cell Biol.*, **44**, 738–747.
78. Kim, K.M., Noh, J.H., Bodogai, M., Martindale, J.L., Yang, X., Indig, F.E., Basu, S.K., Ohnuma, K., Morimoto, C., Johnson, P.F. *et al.* (2017) Identification of senescent cell surface targetable protein DPP4. *Genes Dev.*, **31**, 1529–1534.